

On the internal structure of asteroids and comets

A. Campo Bagatin

Departamento de Física, Ingeniería de Sistemas y Teoría de la Señal – Universidad de Alicante, P.O. Box 99, E-03080, Spain e-mail: adriano@dfists.ua.es

Abstract.

The overall knowledge on asteroids and comets has changed remarkably in the two last decades, due to Earth-based observations, theoretical and numerical work, and to probe missions. One of the most intriguing and interesting features regarding these objects is related to their internal composition. Small-scale composition is partly revealed by the meteorites found on the Earth surface, but nothing similar is available for large-scale composition. Unfortunately, inspecting the interior of any celestial body is an issue only to be tackled in the future, if ever. At present, the only available evidences on the internal composition of small solar system bodies are necessarily indirect: bulk densities, rotational periods, rare disintegration events of comets, presence of crater chains on planets and satellites, observations of binaries, grooves on well resolved images of asteroids, and asteroid Itokawa. A summary review of today's knowledge on this subject is presented here and theoretical considerations about the relationship between the known fragmentation properties of small bodies and the possible textures of their internal structure is also proposed.

Key words. Asteroids – Comets – Internal structure – gravitational aggregates – rubble piles

1. Introduction

For a long time, asteroids have been –to human perspective– mere spots of light moving in the sky across the stars. The study of the dynamics of their orbits was the only available knowledge about them. In a similar way, comets were studied dynamically and on the basis of the morphology of their comae. A new science started on October 29th, 1991, when the *Galileo* probe took images of the main belt asteroid *951 Gaspra*. For the first time (if we make exception for the two satellites of Mars, considered to be asteroids captured by

the planet), we had the possibility to see what an asteroid looks like, appreciate its shape, measure its size and the number and sizes of its craters. A number of asteroids and comets have been resolved in detail by space probes and radiotelescopes since then, allowing the beginning of a new deal in the study of small solar system objects. This has allowed to estimate probabilities of collision in the main asteroid belt from the number of craters, to study with some detail surface compositions, morphology of craters, rotation rates, surface patterns such as the presence of regolith and, recently, even the texture of surface regolith. This has been an upgrade in small bodies research, never-

Send offprint requests to: A. Campo Bagatin

theless, no direct measurement of the internal structure of asteroids and comets has been possible in this period and limited evidences are at hand.

At the same time, the development of fast microprocessors has helped theorists in their numerical studies of the fragmentation physics by simulating the physical conditions in which asteroids collide and reaccumulate to form gravitational aggregates (GA).

From a theoretical point of view, Jeffreys (1947) and Öpik (1950) introduced the idea that some asteroids and comets may not be solid objects governed only by material strength. Chapman (1978) actually used the term “rubble piles” to indicate the result of the gravitational reaccumulation of the boulders derived from high velocity collisions on asteroids.¹ Whipple BIB and Weissman introduced similar concepts related to the internal structure of comets.

In Sec. 1, nowadays indications about what is the internal structures of small bodies are summarised. Are they mostly GA or monolithic objects? Sec. 2 analyses the ways in which GA can be characterised. A summary of the expected collisional characteristics and responses for GA. In Sec. 4, the problem of what kind of internal structures one may expect for GA is discussed, based on their possible textures. Finally, Sec. 5 outlines what issues should be improved to better understand this important class of solar system bodies.

2. Evidences for gravitational aggregates

The possibility that a large percentage of objects ranging from a few hundreds of meters to around a few hundreds of km, in the solar system, including asteroids and comets, are GA has gained greater acceptance. The reason for

¹ (Geologists suggest that the term “rubble-pile” is a mis-name, as they consider that a pile of rubble is the result of the abrupt breakdown of a structure, like in a landslide or in the crumbling of a building, giving rise to a pile of very small fragments (rubble), this is generally something substantially different from what one expects in the reaccumulation of boulders by self-gravity

this is the mounting evidence from observations that such configurations should be common. Experiments and numerical simulations support that. In what follows an overview of this evidence is provided.

2.1. Observations

Observational evidence for GA comes primarily from direct optical imaging and radar.

1. Comet disruption. The breakup of comets, such as that of Comet Shoemaker-Levy 9 (SL9) passing by Jupiter in 1994, may offer some insight into small body aggregates. In July 1992, SL9 passed very close to Jupiter, well inside the tidal breakup (Roche) limit for unconsolidated water ice (Asphaug & Benz 1996). Scotti & Melosh (1993) estimated the tidal stress on the inferred parent body and found it to be so small ($\sim 10^4$ bar) that the comet was likely an incoherent aggregate of fragments before breakup.

Some other tidal disruptions are known, however: P/Brooks 2 broke into at least eight fragments when it approached within 2 jovian radii of Jupiter in 1886 (Sekanina & Yeomans (1985), various Sun grazers may also have been broken up by tides (Weissman 1980; Sekanina 2000).

Other comet breakups have been observed, apparently caused by spontaneous nucleus splitting (Weissman 1982), as in the case of Comet C/1999 S4 (LINEAR) (Weaver et al. 2001), and –recently– the Comet Schwassmann–Wachmann 3.

2. Low bulk densities. One of the most striking findings in the close observations of asteroids by probes or radar techniques is the apparent low density of some C-class asteroids. Space probe NEAR, on its way to asteroid Eros, passed close enough to asteroid 253 Mathilde (dimensions $66 \times 48 \times 44$ km) to obtain a detailed shape model of the visible portion and a mass estimate of the body, which together imply a bulk density of 1.3 ± 0.2 g/cm³ (Yeomans et al. 1997;

Veveřka et al. 1997, 1999; Thomas et al. 1999; Cheng 2002). If Mathilde consists mostly of chondritic material, then the effective porosity is around 40%. As discussed above, porosities of 20-40% can result if a body is completely shattered and reassembled, creating a GA. There have been several other recent asteroid density measurements, some owing to advances in groundbased observation (cf. Merline et al. (2002)). A summary of estimated asteroid bulk-densities is presented in Fig. 1 (from Britt et al. (2002)) and in Hilton (2002).

Some S-class asteroid densities have been measured by spacecraft: $2.6 \pm 0.5 \text{ g/cm}^3$ for 243 Ida (Belton et al. 1995), thanks to the discovery of its satellite Dactyl by the Galileo spacecraft, and 2.7 g/cm^3 for 433 Eros, by the NEAR Shoemaker orbiter (Cheng 2002). The higher densities imply lower porosities for these asteroids, but the values are not inconsistent with fractured or shattered configurations of low strength (see Sec. 2). Radar, high-resolution optical imaging, and lightcurve observations are also revealing—for the first time—the presence of asteroid satellites, with an extrapolated frequency of a few percent among the mainbelt population and around 10-20% among near-Earth asteroids (Pravec et al. 2002, 2007). Interestingly, Pravec & Harris (2000) find that a significant fraction of the observed (near-Earth) population of fast rotators are binaries. Binaries provide the best possible measure of the primary mass (strictly, the sum of the masses), and together with shape estimates these lead to bulk density determinations, revealing in many cases some surprisingly low values.

Comets also show surprisingly low bulk-densities. Comet Wild 2 is estimated to have a density between 0.360 and 0.760 g/cm^3 (Davisson et al. 2004); Comet Tempel 1, that was the target of the Deep Impact mission in 2004, shows estimated densities around 0.6 g/cm^3 (A'Hearn et al. 2007) (Davisson et al. (2005) estimate a value

of $0.45 \pm 0.25 \text{ g/cm}^3$). Both may be consistent with the model of a mixture of ices and dust pieces, reaccumulated in a GA due to impacts undergone by their parent bodies. Bulk porosities around 40% seem reasonable and in agreement with structural speculations for GA asteroid.

Somewhat lower values are obtained for Comet Borrelly, (Davisson & Gutierrez 2004) estimate a density between 180 and 360 g/cm^3 . Similar values are calculated by Rickman (1990) for Comet Halley ($0.26 \pm 0.15 \text{ g/cm}^3$) and for Comet Churyumov-Gerasimenko (100 to 500 g/cm^3 , Davisson & Gutierrez (2005)). For the latter comets, bulk porosities on the order of 70 to 80% would apply. Probably, at least in these cases, it is necessary to conclude that the fragments that may be forming these GA comets are themselves porous to some degree.

3. Rotations. Measurements of asteroid spin periods from lightcurve analysis have placed interesting constraints on asteroid properties. Pravec & Harris (2000) analyzed data for nearly 800 main-belt, near-Earth, and Mars crossing asteroids. They found that the smallest asteroids (mean diameter D between 0.2 and 10 km, inferred from the mean visual magnitude assuming an average albedo consistent with the asteroid classes studied) have a nearly bimodal distribution of fast and slow rotators, unlike larger asteroids, which have a more Maxwellian distribution of spins. The small, fast rotators typically have small lightcurve amplitudes, indicating a tendency toward spherical shapes. Most importantly, there is a sharp cutoff at 2.2 h: No asteroid larger than 200 m has been observed spinning faster than this limit, which corresponds roughly to the critical breakup period for a strengthless body of bulk density around 3 g/cm^3 (e.g., Weidenschilling (1981)). Since a priori there is no reason why a strong body would be precluded from spinning faster than this limit, the authors conclude that few (if any) asteroids larger than 200 m have tensile strength. Some very small asteroids

($D < 200\text{ m}$) have spin periods as fast as 2.5 min (Pravec et al. 2002); these objects must have some tensile strength, though they need not be monoliths. Some of these conclusions may be partially reconsidered after the discovery few asteroids larger than 200 m with spin rates higher than 2.2 h and the implications of theoretical analysis of strengths in GA (Holsapple et al. 2007).

4. Giant craters. About 50% of small objects imaged to date have craters with diameters on the order of the radius of the object (Thomas et al. 1999). The most intriguing example is 253 Mathilde, which has at least four craters in this category (Veverka et al. 1999; Chapman et al. 1999). The 11 km Stickney Crater on the martian moon Phobos (dimensions $27 \times 22 \times 19\text{ km}$; Asphaug & Melosh (1993); Murchie & Erard (1996)); and possibly the 10 km concavity on the other martian moon, Deimos (mean radius about 6.2 km ; Thomas et al. (1996)). Other examples of giant craters on small bodies imaged by spacecraft include one 23 km crater and five $\sim 10\text{ km}$ craters on S-class asteroid 243 Ida (dimensions $60 \times 26 \times 18\text{ km}$; Belton et al. (1994, 1995); Thomas et al. (1996)); as many as eight $\sim 4\text{ km}$ or larger craters on 951 Gaspra (dimensions $18 \times 11 \times 9\text{ km}$; Belton et al. (1994); Greenberg et al. (1994)).
5. Crater chains (catenae). Linear configurations of up to several tens equally spaced, similarly sized impact craters spread out over tens of kilometers have been observed on the surfaces of planets and satellites. There are about a dozen crater chains on Ganymede and Callisto (Schenk et al. 1996), and even one or two on the Moon (Melosh & Whitaker 1994; Wichman & Wood 1995), that are not likely to be produced by any ejecta allignment in cratering impacts. Melosh & Schenk (1993) and Bottke et al. (1997) have suggested that these catenae are impact signatures of fragment trains. In this scenario, a tidally disrupted body strikes one of the planets moons on the outbound orbit, several hours to a few days after disruption. The spacing of the craters is a function of the somewhat random orientation of the train with respect to the impact surface. The absence of any correlation between the inferred parent body mass and the number of craters in the catena supports the idea that the fragments reaccumulated via gravitational instability just prior to impact (Asphaug & Benz 1996; Schenk et al. 1996).
6. Doublet craters. Roughly 10% of large impact structures on the Earth and Venus, are doublet craters, i.e., well separated pairs of similar size craters that formed simultaneously (Bottke & Melosh 1996a,b). The craters are too separated for their size to have been formed by tidal disruption or aerodynamic breakup of an asteroid just prior to impact, since these forces are not able to impart enough tangential separation during the short time before collision (Melosh & Stansberry 1991). Bottke & Melosh (1996a,b) showed that tidal disruption of a GA –modeled as a simple two-component contact binary– by a terrestrial planet could result in detached components that evolve to larger separation due to repeated distant encounters with terrestrial planets, or through mutual tidal interactions.
7. Grooves. Another feature indicating that the multi-km asteroids we know best are at least partially fractured is the apparently universal occurrence of linear grooves on their surfaces. Grooves are linear depressions that have been observed on every asteroid with high-resolution images: Gaspra (Veverka et al. 1994), Ida (Belton et al. 1994), Eros (Veverka et al. 2001). They are currently believed to form where loose, incohesive regolith drains into underlying gaping fissures (Thomas et al. 1979). Their lengths indicate the lateral continuity of the fissures that underlie them. The fissures may not have been initially formed by impacts, but they probably open every time a large impact jostles the interior of the asteroid, so the grooves may postdate the fissures themselves. Physical experiments suggest that large voids may develop

beneath blocks trapped in the narrow fissures, so the internal void space could be larger. The presence of grooves on an asteroid thus suggests that its interior is coherent but fractured, and so its tensile strength is reduced from that of a pristine body and that there must be voids within the asteroid, increasing its porosity.

8. Asteroid Itokawa. The most striking evidence of GA is probably the observation of asteroid 25143 Itokawa. This small, 320 m diameter S-asteroid –that was visited by the Hayabusa spacecraft in 2006– holds many features that can be suitably explained by a GA structure.

The measured density of Itokawa is consistent with about 40% void space (Abe et al. 2006). With continued seismic shaking from impacts, smaller particles settle to geopotential minima, forming smooth, level-surfaced regions by covering the blocks underneath. This picture (Cheng 2008) predicts that many blocks on the surface of Itokawa should be perched, so that block heights above the surface often compare to or exceed their widths along the surface. Blocks as large as those found on Itokawa could not have formed as impact ejecta on a body of this asteroid's size, and the volume of mobile regolith on Itokawa is too great to be consistent with its craters. Itokawa's volume of gravel-sized regolith is consistent with extrapolation of its boulder size distribution (Saito et al. 2006; Miyamoto et al. 2006), suggesting a fragmentation size distribution. Both of these observations can be explained by a catastrophic disruption scenario for formation of Itokawa. Nevertheless the interior of Itokawa may contain intact fragments that exceed 100 m size. There are possible block alignments over 100 m long which may be the surface expression of an underlying consolidated structure (one with mechanical strength). One block on Itokawa reaches 50 m size and is exposed, so it would not be surprising that an even larger coherent fragment is buried. An interesting structural comparison between aster-

oids Itokawa and Eros can be found in Cheng (2008)

3. Characterisation of the internal structure of gravitational aggregates

In order to address what the internal structure of a GA is, one has first to define what these objects are. Is an object, formed by one single huge fragment with a few small pebbles reaccumulated upon it, a GA? In Campo Bagatin et al. (2001) and in Richardson et al. (2002), a gravitational aggregate was defined to be an object formed by many fragments in such a way that the mass of the largest fragment (M_{LF}) is not larger than half of the mass of the whole object ($M_{G.A.}$), $M_{LF} \leq \frac{1}{2}M_{G.A.}$.

If we wish to visualise what such a threshold-object may look like, we could assume that its fragments have been reaccumulated in a symmetric way upon the largest one, that they are roughly spherical and have the same size, and that they are packed in the most efficient way. In this case we end up with an object whose size is about 25% larger than the largest component.

Three different physical parameters have been used to characterise any GA, apart from the zero-order ones: size and mass.

1. Porosity. This parameter is related to material and bulk density:

$$\begin{aligned} \text{Porosity} &= \frac{\text{total void space}}{\text{bulk volume}} = \\ &= 1 - \frac{\text{bulk density}}{\text{material density}} \end{aligned}$$

Porosity is a scale-invariant parameter, in fact, as an example, take a cube of side D and fill it with 8 spheres of diameter $d = D/2$: its porosity is $1 - \pi/6 \approx 0.4764$. Take the same cube and fill it with 10^3 spheres (with $d = D/10$), the object has a totally different structure, but its porosity is still the same. Were the spheres packed in the most efficient way –like cannonballs centred on a cubic lattice, as conjectured by Kepler (and shown in general by

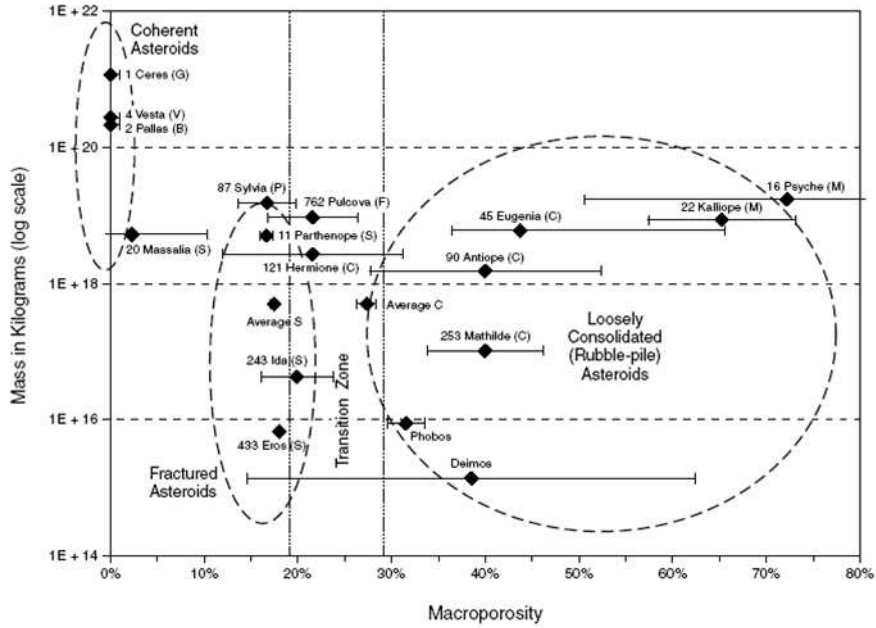


Fig. 1. From Britt et al. (2002). Macroporosities for mainbelt asteroids and TNOs, estimated by subtracting the average porosity of asteroid’s meteorite analogue from the measured bulk porosity.

Hales (1997)– porosity would be 0.2595. Fragments are not usually spherical in real planetesimals and the minimum porosity for arbitrary shaped fragments may be even smaller than that (e.g., it is easy to go below 0.25 for identical ellipsoids [BIBLIO]), however that does not alter the independence of porosity on scale.

2. Relative tensile strength (RTS) (Richardson et al. 2002):

$$RTS = \frac{\textit{Tensile strength of object}}{\textit{Mean tensile strength of components}}$$

Based on porosity and RTS, Richardson built up a characterisation (see Fig. 2) that is useful to distinguish among objects with different physical structures and impact responses.

3. Texture parameter (TP) (Campo Bagatin 2002):

$$TP = \frac{\sum_i \left(\delta_i^3 \frac{M_i}{M_{GA}} \right)}{\sum_i \left(\delta_i^2 \frac{M_i}{M_{GA}} \right)}$$

where, M_i is the total mass of all components of size d_i ; D_{GA} is the size of the GA; M_{GA} its total mass of the GA and $\delta_i = d_i/D_{GA}$ is the relative size of components of size d_i . The TP has the property to take values closer to zero the more the mass distribution is dominated by small components. Instead, as the mass spectrum is dominated by massive components, TP rises towards 1.

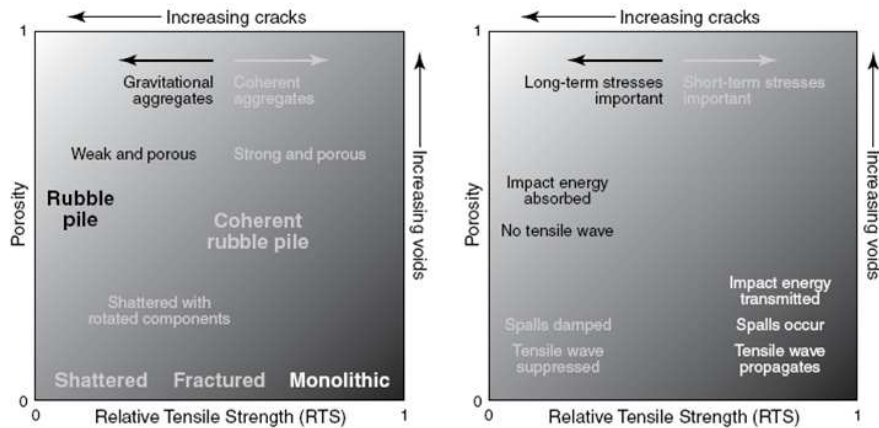


Fig. 2. From Richardson et al. (2002). The RTS-porosity parameter space. The plot on the left assigns labels to distinct regions on the basis of internal structure. The plot on the right describes how objects correspondingly react to stress in these regions. This is a qualitative plot as the quantitative details are poorly known. (From Richardson et al. (2002)).

4. Collisional and tidal behaviour of GA

A GA is produced originally by a former shattering collision on a cohesive parent body. In some case, when the absolute value of the gravitational potential energy of a group of produced and ejected fragments is larger than their kinetic energy, a GA is formed to some extent. The energy condition above is a function of a number of poorly known physical quantities, that may be summarised as: 1) The shattering specific energy Q_S^* , that is the minimum energy per unit mass necessary to disrupt the parent body; 2) The inelasticity coefficient $f_K E$, that is the fraction of relative kinetic energy that goes into fragments; 3) The momentum transference from projectile to targets' components. Q_S^* is estimated in laboratory for targets of many different materials of no more than 20 cm in size. Values for multi-km objects are derived by scaling theories and –alternatively– by numerical experiments mainly based on Smooth Particle Hydrodynamics (SPH) codes. $f_K E$ is estimated in experiments with high uncertain-

ties (0.1 to 0.01). Dependence on momentum has instead not been studied in hiper-velocity collisions.

Not all collisions are shattering events, however, and crater formation occurs when the impact energy is below the threshold limit. Housen (2007) has shown that the effect of n collisions at Q_S^*/n specific energy is approximately equal to the effect of one single Q_S^* impact resulting in a barely shattering of the target. This means that impact after impact the target increases its degree of internal damage –in the sense that the flaws and cracks continue their propagation– until fragments are produced without meaningful jolting of material. A tomography of the structure of such an object would appear mostly like an “Inca wall”, i.e., random assembling of rocks with surfaces matching (and no kind of mortar in between, in the Inca case). In this sense, objects like asteroids Ida, Gaspra and Eros, that do not show low bulk densities, but that do show grooves on their surface, could have this kind of internal structure. It is hard to define such bodies, as they cannot strictly be consid-

ered GA, nor they are coherent bodies even if they may show more tensile strength than GA. Sometimes the term “fractured object” has been used.

Once a GA exists, it can itself be impacted by other bodies and either the dispersion of the GA, either the formation of a second-generation GA may be the consequence. The threshold specific energy for dispersion is often indicated by Q_D^* , the specific energy necessary to disperse more than half of the mass of the former GA. It is obviously impossible, at present, to perform any collisional experiment on a real GA. Nevertheless, some attempt to mimick this situation has been done. Ryan et al. (1991) and Nakamura et al. (1994) investigated the outcome of collisions on targets shattered in a first impact, glue re-assembled by hand and –in the case of ice targets– sintered. In general, the size distribution of fragments after the impact on the re-assembled target did not change much with respect to the one obtained in the first impact, nor large differences in the Q_S^* were found. The situation is slightly better for the study of impacts on porous targets, that may model GA in some case. Davis & Ryan (1990); Nakamura et al. (1992); Ryan et al. (1999); Arakawa et al. (2002); Giblin et al. (2004); Hiraoka et al. (2007); Setoh et al. (2007) performed series of experiments on porous targets of different materials. Even if the details of every experiment may lead to interpretations on side-issues, an overall pattern seems to show up: porous targets are generally harder to disrupt –with respect to non-porous ones– and the ejecta velocities are generally lower with respect to the case of non-porous targets. The effect of gravity cannot be considered in those experiments.

The explanation of the overall collisional trend is in the difficulty of propagation of the shock wave in non-homogeneous or discontinuous media. When a shock wave finds a discontinuity in the material it is propagating in (as in the case of the surface of a fragment), it is reflected back, as no material wave propagates in vacuum. In the case of single fragments in mutual contact, the rebound of the wave at any surface of separation may result

in amplification of its own local damaging effect in the material. In the case of porous but compact targets, instead, it may be the effect is multiple deflections and damping of the wave. The destruction of the target in the collision is then localised near the impact region and the energy residual from dissipation propagates as in partially inelastic collisions, causing the rotation and separation of part of the fragments from the rest, generally at low speeds. In the case of barely fractured objects, the situation is not clear and the reasons for the dissipation of the shock wave presented above may not strictly apply to fragments with contact surfaces. However, dissipation may also appear in these structures, as qualitatively suggested by the historical higher resistance to earthquakes of Inca walls with respect to other kind of building structures based on rock aggregations.

Holsapple et al. (2001, 2004) determined the spin limits of solid bodies without tensile or cohesive strength, but with the pressure induced shear strengths characteristics of dry sands and gravels. Holsapple et al. (2007) gave an extension to that analysis including geological-like materials that also have tensile and cohesive strength. Those strengths are necessary to explain the smaller, fast-rotating asteroids discovered in the last few years. An interesting conclusion of this study is that the spin limits for these more general solids have two limiting regimes: a strength regime for bodies with a diameter $< 3 \text{ km}$, and a gravity regime for the larger bodies with a diameter $> 10 \text{ km}$. The comparison of the theory to the database for the spins of asteroids and TNOs shows good agreement. For large bodies ($D > 10 \text{ km}$), the presence of cohesive and/or tensile strength does not permit higher spin rates than would be allowed for GA. Thus, the fact that the spin rates of all large bodies is limited to periods greater than about 2.2 h does not imply necessarily that they are GA. In contrast, for small bodies ($D < 10 \text{ km}$) the presence of even a very small amount of strength allows much more rapid spins. Small bodies might then be GA but require a small amount of bonding.

Apart from laboratory experiments and theoretical models, numerical experiments

have been performed to try and understand the characteristics of GA.

N-body models have also been used to reproduce the behaviour of GA under tidal influences of close encounters with planets. Some model concentrates on the study of Comet SL9 (Asphaug et al. 1996), while Walsh & Richardson (2006, 2008) study the problem numerically in general. Asphaug & Benz (1994) used an N-body code to model the gravitational forces between the constituent fragments and found that the tidal encounter elongated the rubble pile until a fragment train formed. Tidal breakup simulations of rubble pile asteroids show similar behavior (BIB).

Holsapple & Michel (2006, 2008) give a comprehensive theory that updates the study of the tidal mechanisms acting on cohesionless bodies, including GA.

Other numerical models have studied the fragmentation by means of SPH codes, the subsequent dynamical evolution and mutual gravitational interaction of the fragments resulting from the outcome of this code, have been studied by means of an N-body code (Michel et al. 2004a), and the results of this numerical experiments have been successfully compared to the observed size distribution of some well known asteroid families. This study has been extended to the case of the collisions on pre-fragmented targets (Michel et al. 2004b)

Richardson et al. (2005) studied numerically the behaviour of GA –formed by equal-size spherical masses– that reassemble following a catastrophic disruption, finding that they reconfigure themselves to lie within the stability limits predicted by the continuum theory. Also, coarse configurations consisting of a small number of particles seem to be more resistant to tidal disruption than fine configurations with many particles. Idealised rubble piles seem to behave qualitatively in a manner similar to certain granular materials, at least in the limit where global shape readjustments and/or mass shedding begins.

Numerical hydrocode models of asteroid collisions (Asphaug et al. (1999); ? such as those happened on Phobos, Deimos, Mathilde and probably Gaspra and Ida, suggest that

large craters relative to the body size could have formed only in weak or fragmented targets capable of absorbing the collision energy close to the impact site. A solid monolithic body would have been completely disrupted, erasing any sign of a crater. High-resolution spacecraft observations of some of these bodies support this conclusion. Crater saturation on the surface and the irregular shape of Ida suggest an internal structure that is at least megaregolith or possibly large blocks covered by rubble (Chapman et al. 1996a; Greenberg et al. 1996; Sullivan et al. 1996). Similarly, Gaspra is probably covered with megaregolith but its lumpy structure is also consistent with a blocky interior (Greenberg et al. 1994; Chapman et al. 1996b).

5. Abundances of GA in asteroids and TNOs

Once one assumes that the formation of GA is a common process for objects undergoing catastrophic fragmentation, it is obvious that this kind of structures may be common in collisional systems as the Main Asteroid Belt (MAB) and the Trans-Neptunian populations (TNOs). In order to study the abundance of GA in the MAB, Campo Bagatin et al. (2001) studied the collisional evolution of asteroids taking into account the amount of reaccumulation occurring in any possible collision and keeping track of the number of GA at any size interval as the collisional evolution goes on. As an overall pattern, they found a significant fraction (50 to 100%, depending on different physical assumptions) of objects in the 10 – 100 km size range to be GA. Below 10 km, the fraction decreases to a few percent around 1 km. (Fig. 3) In some simulations, Campo Bagatin et al. (2001) mimicked GA dispersion conditions by lowering f_{KE} by one order of magnitude with respect to monolithic bodies.

Recently, Campo Bagatin and Benavidez (in press) have investigated the abundance of GA in Trans-Neptunian populations using a similar approach. They find that the abundance in GA strongly depends on the scaling-law that has been used to simulate their response to col-

lisions. In some cases, the family of power-laws found by Benz & Asphaug (1999) with an SPH code in numerical experiments, was used for GA. This results in a relatively low ratio of GA (20 to 30% in the 10 – 100 km size range) at the end of the collisional evolution. When other scaling-laws available in literature are used, the abundance of GA in TNO populations reaches 100% in the same range. Again, varying physical assumptions and initial conditions affects mainly the two tails of the abundance-size distribution, that is, below 10 km and above 100 km. (Fig. 4).

6. Does texture matter?

When the bulk density of an asteroid or a comet is measured, an estimation of its porosity may be provided easily. As shown in Sec. 2, different textures are possible for a single porosity value. This means that many different solutions for the mass spectrum of the constituting fragments may apply. In principle, the body may be an aggregate of tiny fragments (that would imply a low texture parameter, TP), an aggregate of a few large fragments (high TP), or rather an object formed by a largest block and many fragments in a whole range of sizes down to gravel, in a way similar to that extrapolated from laboratory experiments (In this case, the value of the TP would depend on the size of the largest fragment relatively to the whole GA). Without any insight in the interior of any small solar system body, only statistical considerations can be done. On one hand, from the results of experiments, and from scaling theories, the threshold specific energy for shattering for a given cohesive target may be derived. For a given relative velocity of impact, the size of the smaller shattering projectile can be found. Moreover, scaling theories provide the size of the largest fragment produced in any collision and the size distribution of fragments, laboratory experiments provide clues to the mass-velocity dependence of ejected fragments. Numerical codes have been developed to infer –using that information– the amount of mass and the size distribution of the fragments of a gravitationally reaccumulated object. On the other hand, by means of a collisional evo-

lution algorithm it is possible to compute how many projectiles of any size can impact a given target within a given interval of time. The size distributions of objects in a collisional system like the MAB, the Trojan swarms or the trans-Neptunian regions, are represented by power-laws with negative exponents that may vary at different size intervals. This generally means that small objects are far more numerous than larger ones at any size, and therefore can collide more frequently with any given target with respect to larger projectiles. All that leads to the conclusion that barely shattering collisions are more common than highly energetic collisions, assuming the relative velocities of impact around average values. In this sense, high TP textures should be more common than low TP ones, and GA made of a largest fragment with a mass slightly smaller than half of the overall body (this is the definition of a “threshold” GA) would be the most common –somewhat contrarily to the standard idea of what a “pile of rubble” is. The quantitative result of this calculations vary depending on the size of the objects one is interested on and on the specific collisional system. In the case of the Asteroid Belt, 90–95% of 1 km GA result from the reaccumulation of barely shattered parent bodies and have high TP values. This abundance decreases to 70 – 75% in the case of 100 km GA. Nevertheless, the scaling laws and the fragments’ mass distribution in hyper-velocity collisions may differ from what outlined above. For instance, the effect shown by Housen (2007) may alter significantly the mass spectrum of the produced fragments and the texture of the GA produced by a secondary impact on a pre-shattered body. SPH numerical experiments show fragmentation patterns for multi-km targets that suggest a high amount of damage in the target material with the formation of similar size fragments close to the resolution of the code itself. In this case, the formation of GA with low values of the TP is in order, contrarily to the classical fragmentation scheme outlined above.

The issue of the texture of GA may be relevant in many ways. Little is known about the response of GA to impacts, the way energy and momentum do propagate in the target compo-

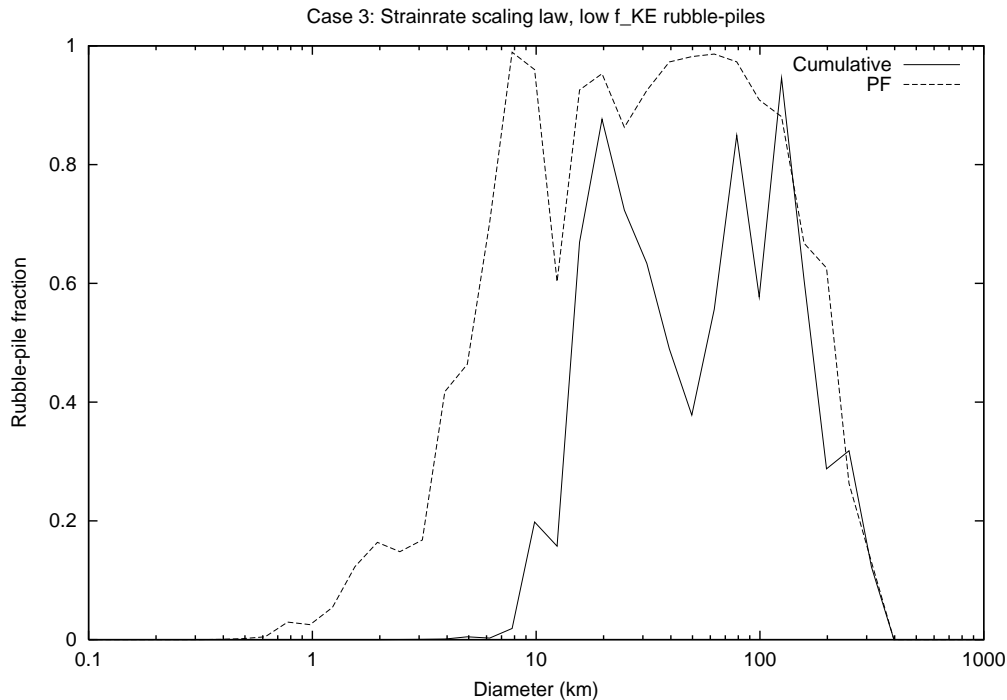


Fig. 3. From Campo Bagatin et al. (2001). GA abundances ('Rubble-pile fraction', in the figure vertical label) for the MAB. The fraction of GA –distinguishing the case in which a relationship suggested by experiments applies between ejection velocity of fragments and their mass (PF) is accounted for– and the standard case. GA are considered as having the anelasticity coefficient f_{KE} 1 order of magnitude smaller with respect to monolithic bodies.

nents after a collision may depend on the number and masses of components so that different textures for a given mass target may result in different patterns of collisional dispersion of the components. This has implications in a variety of planetary research fields. 1) The study of the accumulation of mass in planetary formation mechanisms; 2) The understanding of tidal disruption of asteroids and comets in close planetary encounters; 3) The set up of strategies of mitigation of the hazard due to the risk of asteroidal impacts on Earth.

7. Discussion

A review of the main evidences about the existence of GA among asteroids and comets has been presented. The existence of at least

one such object (asteroid Itokawa) seems to be clear.

Numerical studies of the collisional evolution of the asteroid belt and the trans-Neptunian regions allow rough estimates about the abundance of GA structures in those populations. As those estimates depend upon the mass spectrum of fragments created in shattering impacts, better estimates of the abundances shall be available once the processes of fragmentation of asteroidal-size bodies will be better understood. Even if little is known about the way GA respond to collisions, the development and availability of fast computers is increasing the possibilities that theoreticians have to check the processes that involve GA when they are affected by impacts. Considering the effects of mutual friction among fragments is also necessary to develop correct numerical ex-

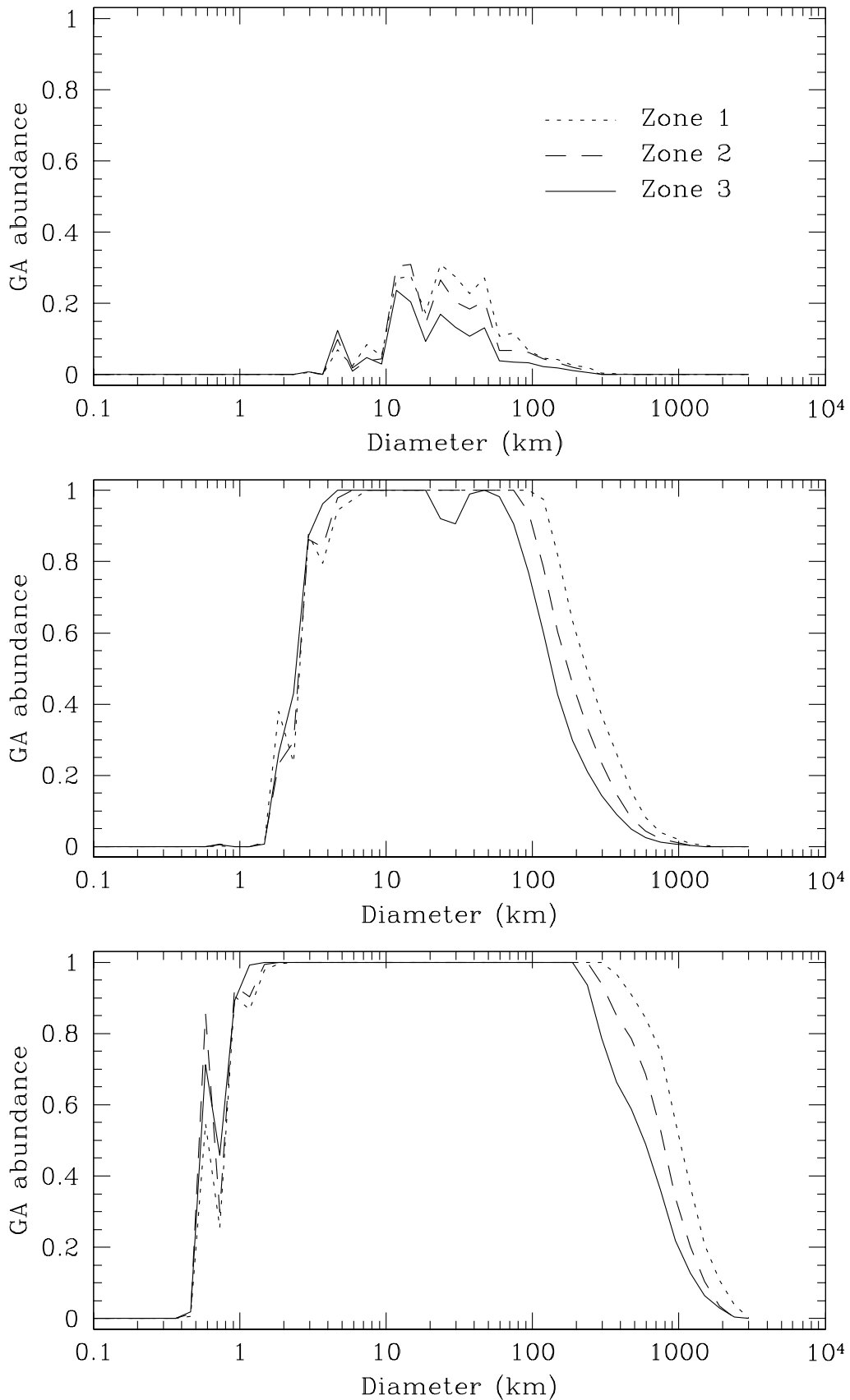


Fig. 4. From Campo Bagatin (2008). Fraction of GA resulting in the collisional evolution of the three TNOs dynamical regions considered in the model (Zone 1 is for 'Plutinos', Zone 2 for Classical Disk objects, and Zone 3 for Scattered Disk objects). The upper figure shows the abundance in the case of a scaling law assuming self-compression due to gravity, but no strain-rate effect leading to a decrease in Q_5^* with size; the middle figure assumes a shallow strain-rate effect, while lower figure assumes higher degree for this effect. GA are always considered as having a Q_5^* like in Benz & Asphaug (1999).

periments. Numerical studies of the shattering threshold energies at different sizes and their dependence on the texture of GA are at an infant state. Rotation is another issue to be included into such studies.

However, the deepest understanding of actual internal structures of small bodies will be at hand only if real object shall be studied in this sense. Tomography and sismography of NEAs are needed: future missions to asteroids or comets should include devices able to perform measurements of the internal structure at some extent. Answering to questions like what the texture of an NEA is, may reveal to be a main issue in the mitigation of the risk of impact on Earth by an asteroid. Science is often costly, but to avoid answering key questions of Nature always turns out into a much higher cost.

Acknowledgements. I acknowledge the Spanish Ministerio de Educación y Ciencia, that supports this investigation under the national project AYA2005-07808-C03-03.

References

- Abe, S. 2006, *Science*, 312, 1344.
 A'Hearn, M. et al. 2007, *Science*, 310, 258.
 Arakawa, M. et al. 2002, *Icarus*, 158, 516.
 Asphaug, E. 1996, *Icarus*, 121, 225.
 Arakawa, M., Melosh, H.J. 1993, *Icarus* 101, 144.
 Asphaug, E., Benz, W. 1994, *Nature* 370, 120.
 Asphaug, E., Benz, W. 1996, *Icarus*, 121, 225.
 Asphaug, E., Scheeres, D.J. 1999, *Icarus*, 139, 383.
 Asphaug, E., Agnor, C. 2005, AAS DPS meeting Bull. A.A.S., 37, 623.
 Belton, M.J. 1994, *Science*, 247, 1647.
 Belton, M.J. 1995, *Nature*, 374, 785.
 Benz, W., Asphaug, E. 1999, *Icarus*, 142, 5.
 Bottke, W.F., Melosh, H.J. 1996, *Nature*, 381, 51.
 Bottke, W.F., Melosh, H.J. 1996, *Icarus*, 124, 372.
 Bottke, W.F. et al. 1997, *Icarus*, 126, 470.
 Britt, ., Consolmagno, G. 2002, In Asteroids III, UAP, 485.
 Campo Bagatin, A. et al. 2001, *Icarus*, 149, 198.
 Campo Bagatin, A. 2002, *Proc. ACM* 2002, 729.
 Campo Bagatin, A., Benavidez, P. 2008, *Icarus*, in press.
 Chapman, C.R. 1978, In Asteroids, UAP, 145.
 Chapman, C.R. et al. 1996, *Icarus*, 120, 77.
 Chapman, C.R. et al. 1996, *Icarus*, 120, 231.
 Chapman, C.R. et al. 1999, *Icarus*, 140, 28.
 Cheng, A.F. 2002, In Asteroids III, UAP, 351.
 Cheng, A.F. 2008, *Planet. Space Sci.*, in press.
 Davidsson, B.J.R. et al. 2005, *Icarus* 191, 547.
 Davidsson, B.J.R., Gutierrez P.J. 2004, *Icarus*, 168, 392.
 Davidsson, B.J.R., Gutierrez P.J. 2005, *Icarus*, 176, 453.
 Davidsson, B.J.R. et al. 2004, AAS DPS meeting; Bull. of the AAS, 36, 1118.
 Davis, D.R. 2002, *Icarus* 83, 156.
 Giblin, I. et al. 2004, *Icarus*, 171, 487.
 Greenberg, R. et al. 1994, 107, 84.
 Greenberg, R. et al. 1996, 120, 106.
 Hales, T.C. 1997, *Discrete Computational Geometry*, 17, 1.
 Hilton, J.L. 2002, In Asteroids III, UAP, 103.
 Hiraoka, K. 2007, *Advances in Space Research*, 39, 392.
 Holsapple K.A. 2001, *Icarus*, 154, 432.
 Holsapple K.A. 2004, *Icarus*, 172, 272.
 Holsapple K.A. 2007, *Icarus*, 187, 500.
 Holsapple K.A., Michel, P. 2008, *Icarus*, 183, 331.
 Holsapple K.A., Michel, P. 2008, *Icarus*, 193, 283.
 Housen, K. 2007, *Lunar and Planetary Science. LPI Contribution 1338*, 1462.
 Jeffreys, H. 1947, *MNRAS*, 107, 260.
 Melosh, H.J., Schenk, P. 1993, *Nature*, 365, 731.
 Melosh, H.J., Stanberry, J.A. 1991, *Icarus*, 94, 171.
 Melosh, H.J., Whitaker, E.A. 1994, *Nature*, 369, 713.
 Merline, W.J. et al. 2002, In Asteroids III, UAP, 289.
 Michel, P. et al. 2004 *Planet. Space Sci.*, 52, 1109.
 Michel, P. et al. 2004, *Icarus*, 168, 420.
 Miyamoto, H. et al. 2004 *Lunar and Planetary Science XXXVIII*, LPI Contribution 1338, 1614.

- Murchie, S., Erard, S. 1996, *Icarus*, 123, 63.
- Nakamura, A. et al. 1992, *Icarus*, 100, 127.
- Nakamura, A. et al. 1994, *Planet. Space Sci.*, 42, 1043.
- Öpik, 1947, *Irish Astronomical Journal*, 1, 25.
- Pravec, P. et al. 2002, In *Asteroids III*, UAP, 113.
- Pravec, P., Harris, A.W. 2007, *Icarus*, 190, 250.
- Pravec, P., Harris, A.W. 2000, *Icarus*, 148, 12.
- Richardson D.C. et al. 2002, In *Asteroids III*, UAP, 113.
- Richardson D.C. et al. 2005, *Icarus*, 173, 349.
- Rickman, H. 1990, in *Comet Halley*, ed. J. W. Mason (Ellis Horwood, New York), 2, 163
- Ryan, E.V. et al. 1991, *Icarus*, 84, 283.
- Ryan, E.V. et al. 1999, *Icarus*
- Saito, J. 2006, *Science*, 312, 5778.
- Schenk, P.M. et al. 1996, *Icarus*, 121, 249.
- Scotti, J.V., Melosh, H.J. 1993, *Nature*, 365, 733.
- Sekanina, Z., Yeomans, D.K. 1985, *Astron. J.*, 90, 2335.
- Sekanina, Z. 2000, *Astrophys. J. Lett.*, 542, L147.
- Setoh, m. 2006, *Earth Planets and Space*, 59, 319.
- Sullicvan, R. 1996, *Icarus*, 120, 119.
- Thomas, P.C. et al. 1979, *J. Geophys. Res.*, 84, 8457.
- Thomas, P.C. et al. 1996, *Icarus*, 123, 536.
- Thomas, P.C. et al. 1999, *Icarus*, 142, 89.
- Veverka, J. et al. 1994, *Icarus*, 107, 72.
- Veverka, J. et al. 1997, *Science*, 278, 2109.
- Veverka, J. et al. 1999, *Icarus*, 140, 3
- Veverka, J. et al. 2001, *Science*, 292, 484.
- Walsh, K.J., Richardson, D.C., *Icarus*, 180, 201.
- Walsh, K.J., Richardson, D.C., *Icarus*, 193, 553.
- Weaver H.A. et al. 2001, *Science*, 292, 1333.
- Weidenschilling, S.J. 1981, *Icarus*, 46, 124.
- Weissman, P.R. 1980, *Astron. Astrophys.*, 85, 191.
- Weissman, P.R. 1980, *GSA special paper*, 190, 14.
- Wichman, R.W., Wood, C.A. 1995, *Geophys. Res. Lett.*, 22, 583.
- Yeomans, D.K. et al. 1997, *Science*, 289, 2085.